INTERNATIONAL SOCIETY FOR SOIL MECHANICS AND GEOTECHNICAL ENGINEERING

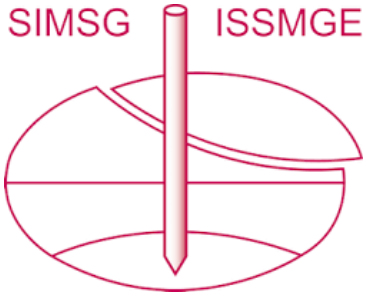

This paper was downloaded from the Online Library of the International Society for Soil Mechanics and Geotechnical Engineering (ISSMGE). The library is available here:

https://www.issmge.org/publications/online-library

This is an open-access database that archives thousands of papers published under the Auspices of the ISSMGE and maintained by the Innovation and Development Committee of ISSMGE.

The paper was published in the proceedings of XVI Pan-American Conference on Soil Mechanics and Geotechnical Engineering (XVI PCSMGE) and was edited by Dr. Norma Patricia López Acosta, Eduardo Martínez Hernández and Alejandra L. Espinosa Santiago. The conference was held in Cancun, Mexico, on November 17-20, 2019.

Geotechnical Engineering in the XXI Century: Lessons learned and future challenges
N.P. López-Acosta et al. (Eds.)

© 2019 The authors and IOS Press.
This article is published online with Open Access by IOS Press and distributed under the terms of the Creative Commons Attribution Non-Commercial License 4.0 (CC BY-NC 4.0).
doi:10.3233/STAL190076

Behavior of a Single-Helix Anchor in Sand Subjected to Cyclic Loading: Centrifuge Modeling

José A. SCHIAVON[a,1], Cristina de H. C. TSUHA[b] and Luc THOREL[c]
[a] *Aeronautics Institute of Technology, Brazil*
[b] *University of São Paulo, Brazil*
[c] *IFSTTAR, France*

Abstract. This paper presents an evaluation of the behavior of a single-helix anchor in very dense sand subjected to cyclic loading via centrifuge tests. To achieve the centrifuge results comparable to the full-scale tests, a verification of scale effects on the uplift capacity of screw anchor models was carried out before the cyclic tests. For this evaluation, anchor models with different dimensions were tested to simulate the same prototype with a helix embedment depth of 6 times the helix diameter (6*D*). The results indicate no scale effect for the range of models investigated. In case of the cyclic tests, two anchor models (one instrumented) installed at 7.4*D* helix embedment depth were tested up to 3000 cycles of loading. The pre-stressing load (minimum cyclic load) showed to have some influence on the cyclic displacement accumulation. Depending on the load amplitude, no trend of stabilization was observed in further cycles. In addition, the post-cyclic monotonic capacity was apparently not influenced by the loading cycles.

Keywords. helical anchors, cyclic loading, sand, centrifuge modeling.

1. Introduction

Helical anchors are normally used to support structures, such as transmission towers, submerged pipelines, decks, solar panels etc. More recently, attention has been given to helical anchors for offshore application, such as jacket and floating structures to support wind turbines. In these cases, during its service life, the foundation is subjected to repeated loading, which may cause changes in the soil condition close to the anchor, and consequently, performance of the helical anchor may be affected.

In sand, the installation of helical anchors disturbs the in-situ soil condition. As the anchor is screwed into the ground, the helices shear and displace the soil laterally, and to a lesser extent in upward direction. This causes density change of the sand in the cylinder circumscribed by the helices [1]. In addition, the sand outside the cylinder is displaced away from the helix radially, which causes compaction and increase of lateral stresses [2]. Figure 1 shows a cross-sectional image of a micro-tomographic analysis of sand specimen after the installation and pullout (10 mm i.e 0.5*D* in model scale) of a

[1] Corresponding author, Civil Engineering Division, Aeronautics Institute of Technology – ITA, Praça Marechal Eduardo Gomes, 50, São José dos Campos, 12228-900, SP, Brazil; E-mail: schiavon@ita.br.

plastic helical anchor. Darker shades of grey correspond to disturbed zone of sand caused by the penetration of helix and shaft found to have greater degree of voids [3].

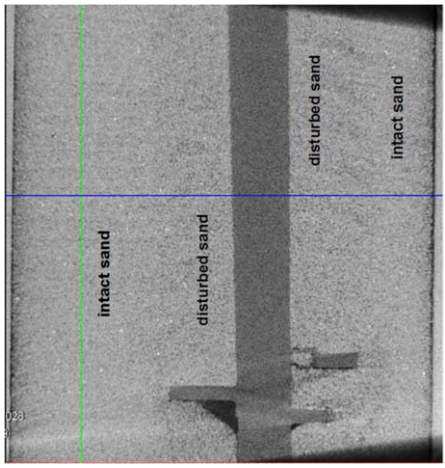

Figure 1. Longitudinal cross-section of plastic model anchor in sand using micro-tomographic [3].

The anchor capacity is a combination of the helix bearing resistance and the shaft resistance [4]. Normally, the bearing resistance is the predominant portion of the total capacity. Under repeated loads, the disturbed sand in the cylindrical zone above the helices may experience compaction, which depends on the amplitude of the anchor movement and the number of repetitions. Consequently, the lateral stresses in the sand outside the cylindrical zone may decrease and some reduction of uplift capacity may occur. More importantly, the continuing anchor upward movement leads to the development of a cavity below the helices and shaft tip. In the case of expected inflow of sand into the cavity, significant reduction in anchor capacity may occur [5].

Newgard *et al*. [6] observed complete pullout after 9500 low-amplitude load cycles on a shallow helical anchor in medium dense sand. The authors point the need for a better understanding on the movements of a helical anchor at failure induced by cyclic loading. To avoid the pullout failure, it is recommended to ensure in design that the tensile cyclic loads are below 60-70% of the anchor uplift capacity Q_T [7]. In addition to anchor pullout due to cyclic loading, excessive anchor uplift may lead to instability of the superstructure. A general recommendation is to keep cyclic loads below 25% of Q_T to minimize long-term creep [8] [9].

Buhler & Cerato [10] observed improvement in the uplift capacity when the helical anchor in sand was subjected to a series of two cyclic loads with 33-39% and 33-65% of the predicted uplift capacity. According to these authors, the densification of the soil above the helices during the cyclic loading is the most likely effect to explain the capacity increase. In addition, the cyclic load amplitude was observed to cause more influence on the anchor response rather than in the maximum load.

Despite the above recommendations, the current understanding on the behavior of helical anchors under cyclic loading is still scarce and few information for the design are available in the literature. The rate of displacement accumulation changes with the cyclic load amplitude as well as with the number of cycles. In addition, degradation of the post-

cyclic monotonic capacity may occur according to the amplitude and number of cycles. To understand the above mechanism in prototype condition, physical modeling of helical anchors in very dense dry sand was carried out using a geotechnical beam centrifuge.

2. Experimental program

In centrifuge modeling, the intensity of the gravitational field produced by the centrifugal acceleration must be inversely proportional to the reduction scale of the manufactured model. According to scaling laws, for a $1/n$ scaled model the applied centrifuge acceleration should be n times the Earth's gravity. Suitable scaling factor must be considered for a given physical parameter to satisfy fundamental laws of dynamics and, therefore, to achieve similarity between model and prototype [11].

The experiments were undertaken using the IFSTTAR geo-centrifuge in a rectangular container having internal dimensions of 1200 mm × 800 mm × 360 mm (length, width and depth). A screw pile servo-actuator was used for the installation and load tests, both carried out in flight (under macrogravity). Axial forces (Q) and displacements (U) were monitored using force and displacement transducers during installation and load testing, and the installation torque was monitored using a torquemeter. Additional details about the experimental procedure can be found in [12].

The installation of anchor models was carried out at a constant rotation rate of 5.3 rpm, with a constant vertical feed rate equals to one helix pitch per revolution. Each test location was at least 10 times the helix diameter (D) far from the container boundary and from the location of other tests.

The model anchors were tested in dry sand bed that was prepared via dry sand pluviation, in which an automatic hopper passes over the container while the sand pours through a slot to produce a uniform sand rain. The sand used in the centrifuge tests is the dry fraction HN38 of Hostun sand, which is an angular to subangular silica sand having mean grain-size (d_{50}) of 0.12 mm and coefficient of uniformity (C_U) of 1.97 [12].

2.1. Experiments on grain-size effects

Appropriate relationship between model and grain size must be ensured to properly simulate the prototype anchor-soil interaction and to avoid the scaling effect. Therefore, an investigation was carried out to finalize the dimensions of the model anchors to be used in the load tests. The "modeling of models" technique was used for this investigation. In this technique, scale effects are neglected for a large-scale model. Different sizes of models and g-levels are used to simulate the same prototype. Full similarity between model and prototype is achieved when identical non-dimensional response is observed between them.

Four single-helix anchor models of different sizes were used to provide a helical anchor prototype with 100 mm shaft diameter (d) and 330 mm helical plate diameter (D/d ratio equals to 3.3). To simulate the same prototype, each model was tested under a different g-level: 16.7, 12.5, 10 and 8×g, respectively for models H18, H25, HA33 and HA40. The four model anchors used in this experiment are shown in Figure 2. The HA18 model differs from the others because it was fabricated to be used in a previous research [13], while the other models were fabricated especially for the current investigation. The

model anchors were tested with a helix depth $H = 6D$ (1.98 m depth in prototype scale) in a sand bed produced with relative density (D_r) of 99%.

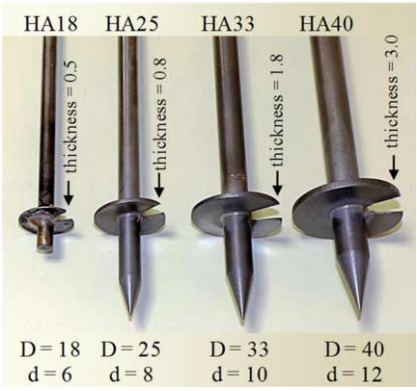

Figure 2. Helical anchor models (dimensions in mm).

2.2. Cyclic loading tests

Cyclic loading tests with different combinations of load amplitude and number of cycles were performed on model anchor HA33 installed in dry sand with $D_r = 99\%$. The model anchor was tested at a helix embedment depth of $H = 7.4D$, which is $3D$ far from the container bottom, which is the largest helix depth possible to avoid boundary effect.

The cyclic loading was applied following a sinusoidal path, right after the model installation without applying any axial load prior to the cycling. The parameters to define the cyclic loading were the mean cyclic load (Q_{mean}) and cyclic load amplitude (Q_{cyclic}), which are defined in Eq. 1 and 2, respectively. Table 1 summarizes information covering 5 cyclic loading tests.

$$Q_{mean} = \left(Q_{max} + Q_{min}\right)/2 \tag{1}$$

$$Q_{cyclic} = \left(Q_{max} - Q_{min}\right)/2 \tag{2}$$

where, Q_{max} is the maximum cyclic load; Q_{min} is the minimum cyclic load.

Table 1. Characteristics and results of cyclic tests.

Test n.	Q_{mean}/Q_T	Q_{cyclic}/Q_T	Q_{min}/Q_T	Q_{max}/Q_T	N (cycles)
C1	0.28	0.10	0.18	0.38	3000
C2	0.32	0.10	0.22	0.42	2000
C3	0.41	0.10	0.31	0.51	2000
C4	0.47	0.19	0.28	0.66	2000
C5	0.32	0.19	0.13	0.51	2000

3. Results and discussion

3.1. Grain-size effects

For the evaluation of scale effects, the uplift capacity (Q_T) was the peak ultimate force recorded during the pullout tests. A total of 13 uplift tests were carried out, having a minimum of 3 tests for each model. Figure 3a presents the results of Q_T obtained with the four models HA18, HA25, HA33 and HA40. The ratio w/d_{50}, where $w = (D - d) / 2$, as it expresses directly the amount of sand grains in contact with the effective surface of the helix. The variation in the Q_T results probably occurred due to variability in the preparation of the sand beds and may not be attributed to grain-size effects. The w/d_{50} ratios varies from 58 to 117 and, in this range, the nearly horizontal trend line proves negligible effect of particle-size (Figure 3a).

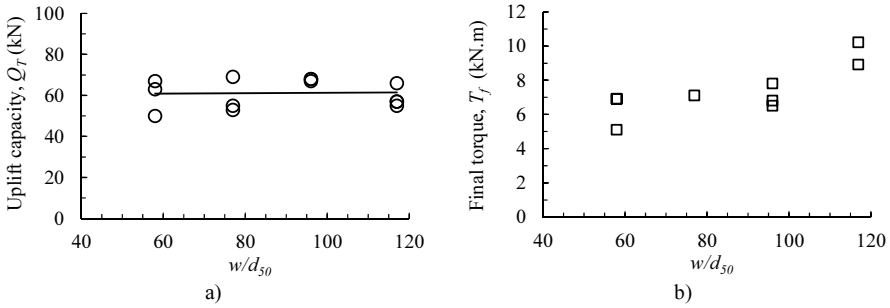

Figure 3. (a) Uplift capacity and (b) final installation torque of models of different sizes.

The installation torque was registered in 9 tests and, therefore, an evaluation of the final installation torque (T_f) was possible. Figure 3b shows that T_f for w/d_{50} ratios 96 and 117 (HA33 and HA40, respectively) is slightly greater than the results found for the other models. Both models HA33 and HA40 were fabricated with a thicker helical plate (18.0 and 25.0 mm thickness in prototype scale, respectively) compared to models 6FH and 8FH (8.4 and 8.8 mm thickness in prototype scale) to avoid plate bending during installation. The thicker the helical plate, the greater the volume of the soil displacement due to the passage of the helix, which increases the installation torque. Therefore, the torque gain observed in models HA33 and HA40 is not due to the scale effect.

3.2. Cyclic loading

In the cyclic study, the cyclic loading parameters (Q_{mean} and Q_{cyclic}) depend on the monotonic uplift capacity (Q_T), which was obtained via uplift loading test using the helical anchor model installed in flight at a helix embedment depth of $H = 7.4D$. In this uplit test, the uplift capacity Q_T, recognized as the ultimate load, was 93 kN, and was used to define the intensity of the load parameters for cyclic test.

The three cyclic loading tests named as C1, C2 and C3 were performed with similar cyclic amplitude ($Q_{cyclic} = 0.10Q_T$) but different mean cyclic load Q_{mean}, which also led to different values of minimum cyclic load (Q_{min}). Those tests aimed to investigate how

the anchor performs under cyclic loading for different levels of pre-stressing load, i.e. Q_{min}. Figure 4a shows that the displacement accumulated (U_{acc}) in the first cycle is significantly larger compared to the rest. The first cycle is the first loading on the disturbed sand above the helix; therefore, the subsequent cycle starts with some sand densification above the helix. Figure 4b shows that the significant displacement accumulation occurs in the first 100 to 300 cycles, which correspond to the phase in which significant sand densification, and therefore, significant volumetric strain occur. Figure 4b also shows that the anchor experienced larger vertical displacements in the test of lower Q_{min} (C1). While the displacement accumulated in tests C2 and C3 was 2.6%D and 3.4%D after 2000 cycles, respectively, the test C1 resulted in double the value of C2 (U_{acc} = 5.2%D). Moreover, the curves of displacements of tests C2 and C3 in Figure 4b suggests a decreasing rate of displacement accumulation with load cycles, which is not the case for test C1, since a linear trend of increase in accumulated displacements can be noticed.

Figure 5a shows that the load-displacement responses of tests C4 and C5 are similar, although the Q_{max} in test C5 is approximately 30% larger than in test C4, which suggests that Q_{cyclic} has greater influence than Q_{max} (both tests were conducted with similar Q_{cyclic}). Figure 5b presents the vertical displacements with cycles of tests C4 and C5. Despite the difference in Q_{min} of test C4 (0.28Q_T) compared to test C5 (0.13Q_T), no significant difference in displacements can be noticed, which contrasts with tests C1, C2 and C3. After 2000 cycles, the model anchor showed accumulated displacements of 7.4%D and 7.8%D, respectively, for tests C4 and C5. These conflicting observations on the displacements of tests C1 to C5 suggest that the influence of Q_{min} on displacement accumulation is more pronounced for cases of low values of Q_{cyclic} compared to Q_{min}, which corresponds to low to low-moderate values of maximum cyclic load (roughly Q_{max} up to 50%Q_T). However, perhaps a greater number of cycles is necessary for some significant difference to be noticed in tests C4 and C5. Figure 5b shows that the displacements in the final 1000 cycles of test C4 seem to accumulate at a greater rate that in test C5, which may indicate a trend of poorer performance for cases of lower Q_{min}.

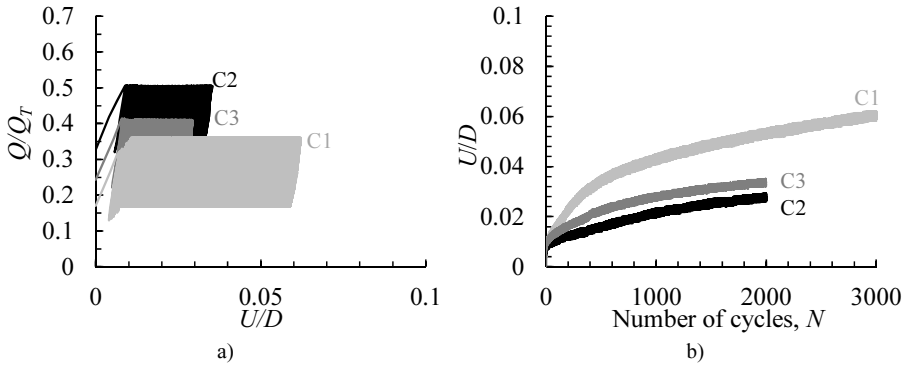

Figure 4. Results of tests C1, C2 and C3: (a) normalized cyclic load-displacement response; (b) displacement response with cycles.

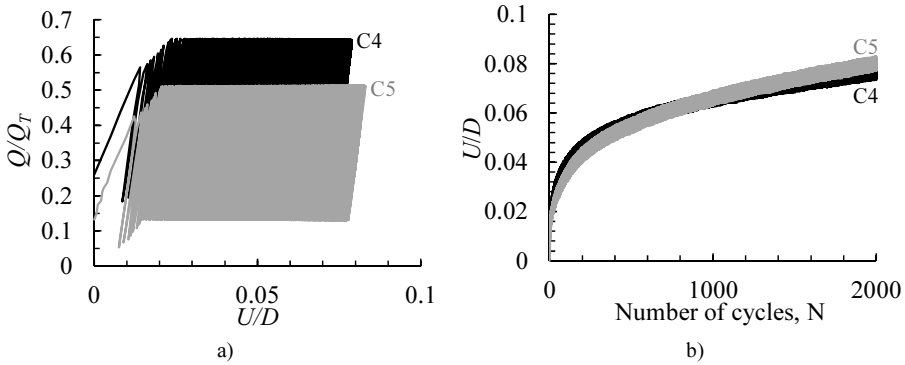

Figure 5. Results of tests C4 and 5 (a) normalized cyclic load-displacement response; (b) displacement response with cycles.

3.3. Post-cyclic monotonic tests

Monotonic pullout tests were carried out after the cyclic tests C2, C3, C4 and C5 to evaluate the occurrence of reduction of post-cyclic uplift capacity ($Q_{T\text{-}pc}$). Figure 6 shows the post-cyclic load-displacement response of these tests. A maximum of 7% reduction in post-cyclic uplift capacity was observed in the current tests, which is considered negligible.

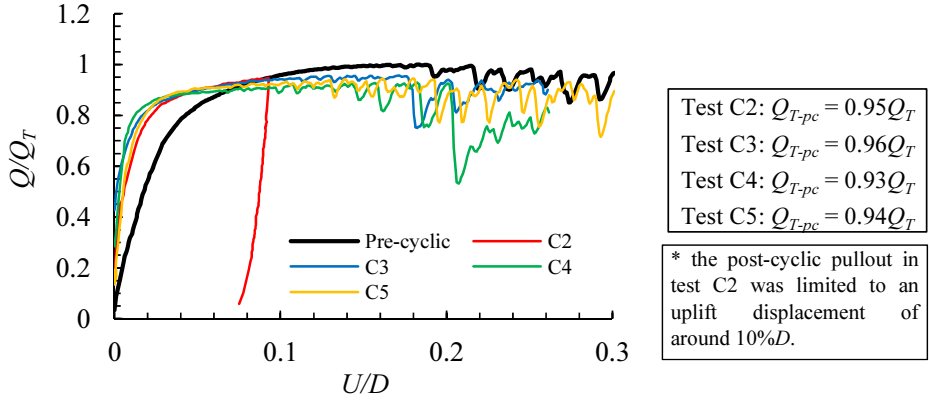

Figure 6. Pre-cyclic and post-cyclic monotonic load-displacement responses.

4. Conclusion

A centrifuge investigation on scale effects and cyclic loading on helical anchor models is presented in this paper. It is observed that the prototype uplift capacity is comparable for w/d_{50} ratio greater than 58. Under cyclic loading the displacement accumulation has significant dependence on the pre-stressing load (Q_{min}) for low to medium-low cyclic amplitudes leading to values of Q_{max} up to ~50%Q_T. Negligible dependence was observed

for medium-high cyclic amplitudes (Q_{max} greater than ~50%Q_T). In post-cyclic uplift, the model anchor exhibited negligible reduction in the uplift capacity for the tested range of Q_{mean}, Q_{cyclic} and number of load cycles (N).

References

[1] Y.U. Sharif *et al*., Numerically modelling the installation and loading of screw piles using DEM. In *Proceedings of the 1st International Symposium on screw piles for energy applications* (2019), 101-108, University of Dundee, Dundee, Scotland.

[2] M.P. Mitsch & S.P. Clemence, The uplift capacity of helix anchors in sand, In *Uplift Behavior of Anchor Foundations in Soil* (1985), 26-47, ASCE, Michigan, USA.

[3] J.A. Schiavon, *Behaviour of helical anchors subjected to cyclic loadings,* PhD thesis, University of São Paulo, São Carlos, Brazil, 2016.

[4] A.J. Lutenegger, Uplift of shallow single-helix screw-piles. In *Proceedings of the 1st International Geotechnical Symposium on Helical Foundations* (2013), 200-210, International Society for Helical Foundations, Amherst, USA.

[5] S.P. Clemence & A.P. Smithling, Dynamic uplift capacity of helical anchors in sand. In *Proceedings of the 4th Australia-New Zealand Conference on Geomechanics* (1984), **1**, 88-93, Australian Geomechanics Society and New Zealand Geomechanics Society, Perth, Australia.

[6] J.T. Newgard *et al*., Cyclic response of shallow helical anchors in a medium dense sand. In *Proceedings of the 3rd International Symposium on Frontiers in Offshore Geotechnics* (2015), **1**, 913-918, Taylor & Francis, Oslo, Norway.

[7] Y.G. Trofimenkov & L.G. Mariupol´skii, Screw piles as foundations of supports and towers of transmission lines, *Soil Mechanics and Foundation Engineering* **1-4** (1964), 232-239.

[8] A.B. Cerato & R.T. Victor, Effects of long-term dynamic loading and fluctuating water table on helical anchor performance for small wind tower foundations, *Journal of Performance of Constructed Facilities* **23-4** (2009), 251-261.

[9] A.M. Ghaly & S.P. Clemence, Pullout performance of inclined helical screw anchors in sand. *Journal of Geotechnical and Geoenvironmental Engineering* **124-7** (1998), 617-627.

[10] R. Buhler & A.B. Cerato, Design of dynamically wind-loaded helical piers for small wind turbines. *Journal of Performance of Constructed Facilities* **24**-4 (2010), 417-426.

[11] R.N. Taylor, Centrifuges in modelling: principles and scale effects, *Geotechnical centrifuge technology* (1995), 19-33.

[12] J.A. Schiavon, Experimental Investigation on the Helical Pile Behaviour Under Cyclic Tensile Loading, PhD thesis, University of São Paulo, São Carlos, Brazil, 2016.

[13] C.H.C. Tsuha, Theoretical model to control on site the uplift capacity of helical screw piles embedded in sandy soil [in Portuguese], PhD thesis, University of São Paulo, São Carlos, Brasil, 2007.